

# Emerging $\gamma$ -soft-like spectrum in $^{196}\text{Pt}$ in the SU3-IBM (I)

Tao Wang,<sup>1,\*</sup> Bing-cheng He,<sup>2,†</sup> Chun-xiao Zhou,<sup>3,‡</sup> Dong-kang Li,<sup>1,§</sup> and Lorenzo Fortunato<sup>4,5,¶</sup>

<sup>1</sup>*College of Physics, Tonghua Normal University, Tonghua 134000, People's Republic of China*

<sup>2</sup>*Physics Division, Argonne National Laboratory, Lemont, Illinois 60439, USA*

<sup>3</sup>*College of Mathematics and Physics Science, Hunan University of Arts and Science, Changde 415000, People's Republic of China*

<sup>4</sup>*Dipartimento di Fisica e Astronomia "G. Galilei"-Università di Padova, via Marzolo 8, I-35131 Padova, Italy*

<sup>5</sup>*INFN-Sez.di Padova, via Marzolo 8, I-35131 Padova, Italy*

(Dated: March 5, 2024)

**Abstract:** Recently, it has been argued that a spherical-like spectrum emerges in the SU3-IBM, opening up new approaches to understand the  $\gamma$ -softness in realistic nuclei. In a previous paper,  $\gamma$ -softness with degeneracy of the ground and quasi- $\gamma$  bands was observed. In this paper, another special point connected with the middle degenerate point is discussed, which is found to be related with the properties of  $^{196}\text{Pt}$ . This emergent  $\gamma$ -softness has also been shown to be important for understanding the prolate-oblate asymmetric shape phase transition. The low-lying spectra,  $B(E2)$  values and quadrupole moments in  $^{196}\text{Pt}$  are discussed showing that the new model can account for several observed features. This is the first part of the discussions on the  $\gamma$ -soft-like spectrum of  $^{196}\text{Pt}$ .

**Keywords:** SU3-IBM,  $^{196}\text{Pt}$ ,  $\gamma$ -soft-like spectrum

## I. INTRODUCTION

Recently, an extension of the interacting boson model with SU(3) higher-order interactions (SU3-IBM for short) was proposed to describe the spherical-like  $\gamma$ -soft spectra in  $^{110}\text{Cd}$  [1], to explain the puzzling  $B(E2)$  anomaly [2, 3], to discuss the prolate-oblate asymmetric shape phase transition in Hf-Hg region including the  $^{196}\text{Pt}$  [4], and to provide an E(5)-like description for  $^{82}\text{Kr}$  [5]. O(6) higher-order interactions were found to be unable to explain the  $B(E2)$  anomaly [6]. These works imply that the SU(3) symmetry dominates the quadrupole deformation of a nucleus, and the  $\gamma$ -softness in realistic nuclei may be an emergent phenomenon, which has a deep relationship with the SU(3) symmetry.

Cd isotopes show a new  $\gamma$ -soft-like rotational behavior, which is unexpected in standard nuclear structure studies [8–14]. The  $B(E2)$  anomaly also seems uncommon, which rejects conventional theoretical explanations, including the interacting boson model (IBM-2) calculations based on the SkM\* energy-density functional and the symmetry-conserving configuration mixing (SCCM) calculations [15–18]. The successful explanation of these two abnormal phenomena makes the new theory of SU3-IBM very attractive, and further exploration of the applications of the theory becomes very valuable, especially on various  $\gamma$ -soft-like phenomena in nuclear spectra. What needs to be emphasized is that these two anomalous phenomena cannot be explained by the interacting boson model with the O(6)  $\gamma$ -softness [6]. Recent studies on

the prolate-oblate asymmetric shape phase transition revealed that the key ingredient of the new model SU3-IBM is to describe the oblate shape with the SU(3) third-order interaction [4].  $\gamma$ -softness comes from the competition between the prolate shape and the oblate shape, thus in the SU3-IBM the new  $\gamma$ -softness is an emergent phenomenon, which is different from the usual O(6) description [19].

The IBM provides an elegant approach to describe the low-lying collective excited behaviors in nuclear structure [20]. In the simplest IBM-1, the basic building constituents are the  $s$  and  $d$  bosons with angular momentum  $l = 0$  and  $l = 2$  respectively, and the collective states of a nucleus can be spanned by the  $\text{su}(6)$  algebra. Up to two-body interactions, a consistent- $Q$  (CQ) Hamiltonian adopted in this model is [21, 22]

$$\hat{H}_1 = c \left[ (1 - \eta) \hat{n}_d - \frac{\eta}{N} \hat{Q}_\chi \cdot \hat{Q}_\chi \right]. \quad (1)$$

Here  $\hat{n}_d$  is the  $d$ -boson number operator,  $\hat{Q}_\chi = [d^\dagger \times \tilde{s} + s^\dagger \times \tilde{d}]^{(2)} + \chi [d^\dagger \times \tilde{d}]^{(2)}$  is the generalized quadrupole operator,  $N$  is the total boson number,  $c$  is a scale parameter and  $0 \leq \eta \leq 1$ ,  $-\frac{\sqrt{7}}{2} \leq \chi \leq \frac{\sqrt{7}}{2}$  are parameters that allow to span a full range of different nuclear spectra. Although the formalism is simple, it can describe the spherical ( $\eta = 0$ , the U(5) limit), prolate ( $\eta = 1$ ,  $\chi = -\frac{\sqrt{7}}{2}$ , the SU(3) limit), oblate ( $\eta = 1$ ,  $\chi = \frac{\sqrt{7}}{2}$ , the  $\overline{\text{SU}}(3)$  case) and  $\gamma$ -unstable ( $\eta = 1$ ,  $\chi = 0$ , the O(6) limit) nuclei. This Hamiltonian is extensively used in fitting realistic nuclear spectra and discussing the shape phase transitions between different shapes [20–22].

More than a decade ago, one of the authors (L. Fortunato) and his collaborators generalized the simple formalism (1), and a cubic- $Q$  interaction is introduced as

\* suiyeqiaoqiao@163.com

† bhe@anl.gov

‡ zhouchunxiao567@163.com

§ ldk667788@163.com

¶ fortunat@pd.infn.it

follows [23]

$$\hat{H}_2 = c \left[ (1 - \eta) \hat{n}_d - \frac{\eta}{N} (\hat{Q}_x \cdot \hat{Q}_x + \frac{\kappa_3}{N} [\hat{Q}_x \times \hat{Q}_x \times \hat{Q}_x]^{(0)}) \right], \quad (2)$$

where  $\kappa_3$  is the coefficient of the cubic term. In the SU(3) limit, when  $\chi = -\frac{\sqrt{7}}{2}$ , the cubic interaction can describe an oblate shape (SU(3) oblate), which is different from the previous SU(3) oblate shape in Hamiltonian (1). This indicates that the previous description of the oblate shape with SU(3) symmetry can be replaced by the SU(3) symmetry and a new evolutionary path from the prolate shape to the oblate shape can be established within only the SU(3) limit, see the bottom black line in Fig. 1. Thus an analytically solvable prolate-oblate shape phase transitional description within the SU(3) limit can be provided, see Ref. [24], which offers a rare example for finite- $N$  first-order quantum shape transition. The phase transitional point is also a degenerate point [24], which implies a hidden symmetry [1]. This hidden symmetry is responsible for the whole new progress in [1–6]. Moreover, in this extended Hamiltonian  $\hat{H}_2$ , there is only a very tiny region of rigid triaxiality in the large- $N$  limit at  $\chi = -\frac{\sqrt{7}}{2}$  when the parameter changes from the U(5) limit to the SU(3) degenerate point, see the green line in Fig. 1.

These new results presented by Ref. [23, 24] encourage us to understand the existing experimental phenomena from a new perspective. Some new and unexpected results have emerged recently. A new shape triangle can be drawn (see Fig. 1), which is similar to the Casten triangle related to the Hamiltonian (1) [25]. In the SU3-IBM new theory [1], new  $\gamma$ -soft-like triaxial rotation is found, which is different from the O(6)  $\gamma$ -unrelated rotational mode in Hamiltonian (1). The shape transitional behaviors from the U(5) limit to the SU(3) degenerate point was numerically explored (green line in Fig. 1). The key observation is that, spherical-like  $\gamma$ -soft triaxial rotational spectra actually exists (see Fig. 5 (a)), which may be the candidate to solve the spherical nucleus puzzle [11, 12, 26]. Within the parameter region of the green line in Fig. 1, we find the unexpected result that there is an accidental degeneracy of the corresponding energy levels between the ground and quasi- $\gamma$  bands such that they form an exactly degenerate multiplet. It will be clear, from the ensuing discussion, that while this degenerate multiplet corresponds to that found in the SO(5) symmetry with quantum number  $\tau = 2$ , the next one ( $\tau = 3$ ) is not exactly degenerate, a feature that is often observed in actual nuclear spectra.

Historically, higher-order interactions in IBM-1 were introduced to describe  $\gamma$ -rigid triaxial deformation and interactions  $[d^\dagger d^\dagger d^\dagger]^{(L)} \cdot [\tilde{d} \tilde{d} \tilde{d}]^{(L)}$  can play a key role for triaxiality of the ground state [27, 28]. An important progress related with our works is investigating SU(3) symmetry-conserving higher-order interactions [29]. Subsequently, within the SU(3) limit, an algebraic realization of the rigid asymmetric rotor was established [30, 31]. Recently, this realization has been

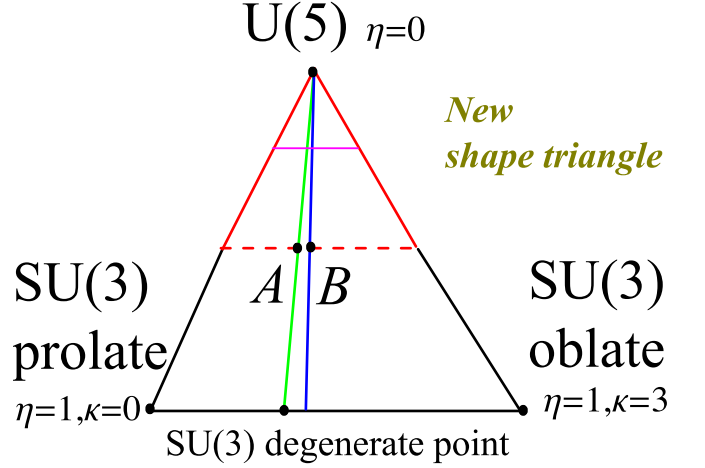


FIG. 1. New shape triangle: the top point of the triangle presents the U(5) limit, which is spherical shape. The two bottom points and the black line between them are all within the SU(3) limit. The left bottom point presents the SU(3) prolate shape, and the right one presents the SU(3) oblate shape.

used to explain the  $B(E2)$  anomaly [3]. SU(3) third-order and fourth-order interactions are also discussed in Ref. [32–35]. Higher-order terms are also important in partial dynamical symmetry [36]. Higher-order interaction  $(\hat{Q}_0 \times \hat{Q}_0 \times \hat{Q}_0)^{(0)}$  can present a rotational spectrum [37], where  $\hat{Q}_0$  is the quadrupole operator in the O(6) limit. This result was further studied by [38, 39]. However the O(6) symmetry was questioned in [6]. In these series of new developments [1–6, 23, 24, 30, 31], SU(3) higher-order interactions begin to show an extremely important role, albeit at a phenomenological level. These higher-order interactions have already been shown to be relevant to some realistic anomalies in nuclear structure [1–3], so introducing these terms is of practical significance.

The  $\gamma$ -soft shape was first described in Ref. [40], where the geometric Hamiltonian is not dependent on the  $\gamma$  variable. In the IBM, the  $\gamma$ -soft case can be described by the O(6) limit [19, 41] and the nucleus of  $^{196}\text{Pt}$  was the first candidate for the O(6) spectra. However there was still some debates about it [42, 43]. In the IBM-2 [20], triaxial shape can be described even with up to two-body interactions [44–47]. Three-body interactions  $[d^\dagger d^\dagger d^\dagger]^{(L)} \cdot [\tilde{d} \tilde{d} \tilde{d}]^{(L)}$  are also used in the IBM-2 to investigate the  $\gamma$  triaxiality [48]. In the sdg-IBM,  $l = 4$  g bosons can be introduced and hexadecapole deformation can be discussed [49]. Except for the IBM, triaxial shapes are also investigated by many existing nuclear models [21, 26, 50–56].

Although  $^{196}\text{Pt}$  seems to adapt to the description in terms of the O(6) symmetry, some noticeable deviations still exist and cannot be described at a satisfactory level in the IBM. The first drawback is that it has a large

electric quadrupole moment [42],  $Q_{21^+}=0.62(8)$ , pointing towards the oblate side. The second is that the staggering feature of  $\gamma$  band breaks the  $O(5)$  symmetry, which seems to be intermediate between the  $\gamma$ -soft and  $\gamma$ -rigid. The third is the positions of the  $0_2^+$ ,  $0_3^+$ ,  $0_4^+$  states, which can not be reproduced well [57].

Recently two important results in the SU3-IBM are also found [4, 5]. In [4], the SU(3)-IBM is used to describe the prolate-oblate shape phase transition with an asymmetric way, which can well explain the shape transitions from  $^{180}\text{Hf}$  to  $^{200}\text{Hg}$  including the nucleus  $^{196}\text{Pt}$ . It was found that, in this shape phase transition, another special point that shows accidental degeneracy features, can be located near the middle of the degenerate line and it can be used to describe the properties of  $^{196}\text{Pt}$  [4]. In [5], a shape transitional behavior like the one from the U(5) limit to the O(6) limit in IBM is found by introducing the SU(3) fourth-order interaction, which can describe the E(5)-like  $\gamma$ -softness in  $^{82}\text{Kr}$ .

Following the ideas of the previous researches, further exploration of the applications of the SU3-IBM is necessary. The  $^{196}\text{Pt}$  is the focus. The three obvious deficiencies discussed above can be well overcome simultaneously. This nucleus is usually regarded as a typical example with O(6) symmetry in Hamiltonian (1). We have found that the new model can give a more reasonable description and our work provides a new understanding for  $\gamma$ -softness in  $^{196}\text{Pt}$  and other similar nuclei, which is related with the SU(3) symmetry. Thus these results in the SU3-IBM ([1–6] and this paper) together confirm the validity of the new idea.

This is the first part of the discussions on the nucleus  $^{196}\text{Pt}$ . In the SU(3) limit, three interactions (the SU(3) second-order Casimir operator  $\hat{C}_2[\text{SU}(3)]$ , the SU(3) third-order Casimir operator  $\hat{C}_3[\text{SU}(3)]$  and the square of the second-order Casimir operator  $\hat{C}_2^2[\text{SU}(3)]$ ) can determine the quadrupole shape of the ground state and the energies of the  $0^+$  states [5]. In this paper, the three operators are first investigated to fit the lowest few  $0^+$  states in  $^{196}\text{Pt}$ . Other three operators  $[\hat{L} \times \hat{Q} \times \hat{L}]^{(0)}$ ,  $[(\hat{L} \times \hat{Q})^{(1)} \times (\hat{L} \times \hat{Q})^{(1)}]^{(0)}$  and  $\hat{L}^2$  can describe the triaxial rotational spectra [30, 31], which will be discussed in the series of following papers.

## II. HAMILTONIAN

### III. $\gamma$ -SOFT-LIKE SPECTRA FOR THE POINT B

In the SU3-IBM, the  $d$  boson number operator  $\hat{n}_d$  must be included, which can describe a spherical shape. This is vital for the pairing interaction between the valence nucleons. Other interacting terms are all SU(3) conserving invariants. The traditional second-order interaction  $-\hat{C}_2[\text{SU}(3)]$  can describe the prolate shape. Ref. [23] pointed out that the third-order Casimir operator

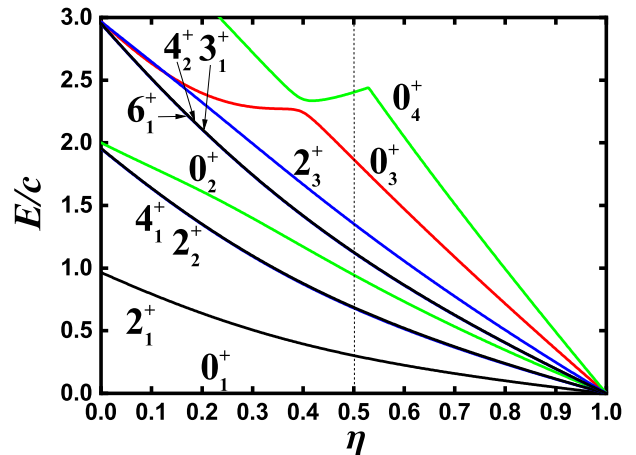


FIG. 2. Partial low-lying level evolution along the green line in Fig. 1 for  $N = 6$ .

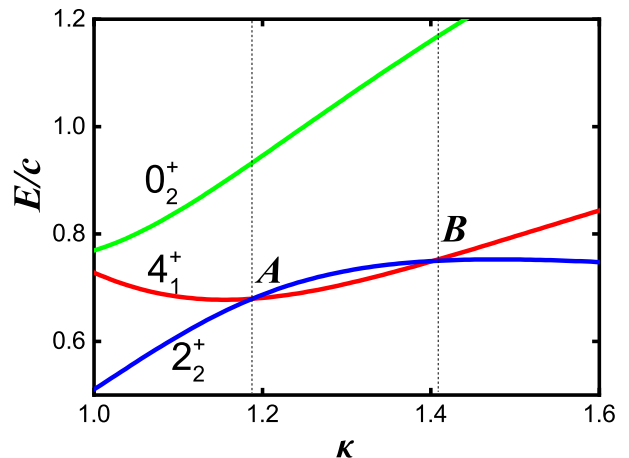


FIG. 3. Level evolution of the  $4_1^+$ ,  $2_2^+$  and  $0_2^+$  states for the parameter  $\kappa$  from 1.0 to 1.6 when  $\eta = 0.5$ ,  $\xi = 0$  and  $N = 6$ . Two crossing points A and B, where accidental degeneracy occurs, can be observed.

$\hat{C}_3[\text{SU}(3)]$  can describe the oblate shape. Other higher-order interactions should be considered in some peculiar phenomena, such as  $B(E2)$  anomaly and some unusual experimental data which can not be described by previous theories [2, 3]. In [5], the square of the second-order Casimir operator  $\hat{C}_2^2[\text{SU}(3)]$  is found to be vital for the  $\gamma$ -softness of the realistic nuclei. In this paper, the third-order invariant operator and the square of the second-order invariant operator are introduced into the interactions, like in Ref. [5] (the fourth-order interaction is only a supplementary term here). Although this is a simple formalism in the SU3-IBM, it shows many new interesting phenomena. Thus the Hamiltonian discussed

in this paper is

$$\hat{H} = c \left[ (1 - \eta) \hat{n}_d + \eta \left( -\frac{\hat{C}_2[\text{SU}(3)]}{2N} + \kappa \frac{\hat{C}_3[\text{SU}(3)]}{2N^2} + \xi \frac{\hat{C}_2^2[\text{SU}(3)]}{2N^3} \right) \right], \quad (3)$$

where  $0 \leq \eta \leq 1$ ,  $c$  is a global energy scale parameter,  $N$  is the boson number,  $\kappa$  is the coefficient of the cubic term,  $\kappa = \frac{9\kappa_3}{2\sqrt{35}}$ ,  $\xi$  is the coefficient of the fourth-order interaction, and  $\hat{C}_2[\text{SU}(3)]$  and  $\hat{C}_3[\text{SU}(3)]$  are the second-order and third-order SU(3) Casimir operators separately. If the fourth-order term is not considered, the Hamiltonian (3) can be described by the new shape triangle in Fig. 1.

In the SU(3) limit the two Casimir operators can be related with the quadrupole second or third-order interactions as following

$$\hat{C}_2[\text{SU}(3)] = 2\hat{Q} \cdot \hat{Q} + \frac{3}{4}\hat{L} \cdot \hat{L}, \quad (4)$$

$$\hat{C}_3[\text{SU}(3)] = -\frac{4}{9}\sqrt{35}[\hat{Q} \times \hat{Q} \times \hat{Q}]^{(0)} - \frac{\sqrt{15}}{2}[\hat{L} \times \hat{Q} \times \hat{L}]^{(0)}. \quad (5)$$

For a given SU(3) irrep  $(\lambda, \mu)$ , the eigenvalues of the two Casimir operators under the group chain  $\text{U}(6) \supset \text{SU}(3) \supset \text{O}(3)$  are given as

$$\langle \hat{C}_2[\text{SU}(3)] \rangle = \lambda^2 + \mu^2 + \lambda\mu + 3\lambda + 3\mu, \quad (6)$$

$$\langle \hat{C}_3[\text{SU}(3)] \rangle = \frac{1}{9}(\lambda - \mu)(2\lambda + \mu + 3)(\lambda + 2\mu + 3). \quad (7)$$

If  $\kappa = \frac{3N}{2N+3}$ , the second term in Hamiltonian (3) describes the SU(3) degenerate point ( $\xi = 0$ ). It should be noticed that the location of the SU(3) degenerate point along the variable  $\kappa$  is related to the boson number  $N$  [4]. For  $^{196}\text{Pt}$ ,  $N = 6$ , it is found at  $\kappa = 1.2$ . In the large- $N$  limit,  $\kappa \rightarrow 1.5$ . At this degenerate point, the SU(3) irreps satisfying the condition  $\lambda + 2\mu = 2N$  are all degenerate.

Fig. 2 presents the partial low-lying level evolutions from the U(5) limit to the SU(3) degenerate point for  $N = 6$  as a function of  $\eta$ . The choice of the boson number  $N = 6$  corresponds to  $^{196}\text{Pt}$ . (In the previous paper [1],  $N = 7$  is discussed for the  $^{110}\text{Cd}$ .) It's clear that the four lowest  $0^+$  states are all degenerate if  $\eta = 1.0$ . The key finding is that the  $4_1^+$  state and the  $2_2^+$  state are degenerate, as well as the triplet of states  $6_1^+$ ,  $4_2^+$ ,  $3_1^+$ . This degeneracy can hold for some higher levels. Unfortunately the reason for this degeneracy is still unknown. This unexpected  $\gamma$ -softness is found in Ref. [1].

The SU(3) degenerate point is found at  $\kappa = 1.2$ . A further exploration around this degenerate point is undoubtedly useful for understanding the new  $\gamma$ -softness. Fig. 3 plots level evolution of the  $4_1^+$ ,  $2_2^+$  and  $0_2^+$  states for the parameter  $\kappa$  from 1.0 to 1.6 when  $\eta = 0.5$ ,  $\xi = 0$  and

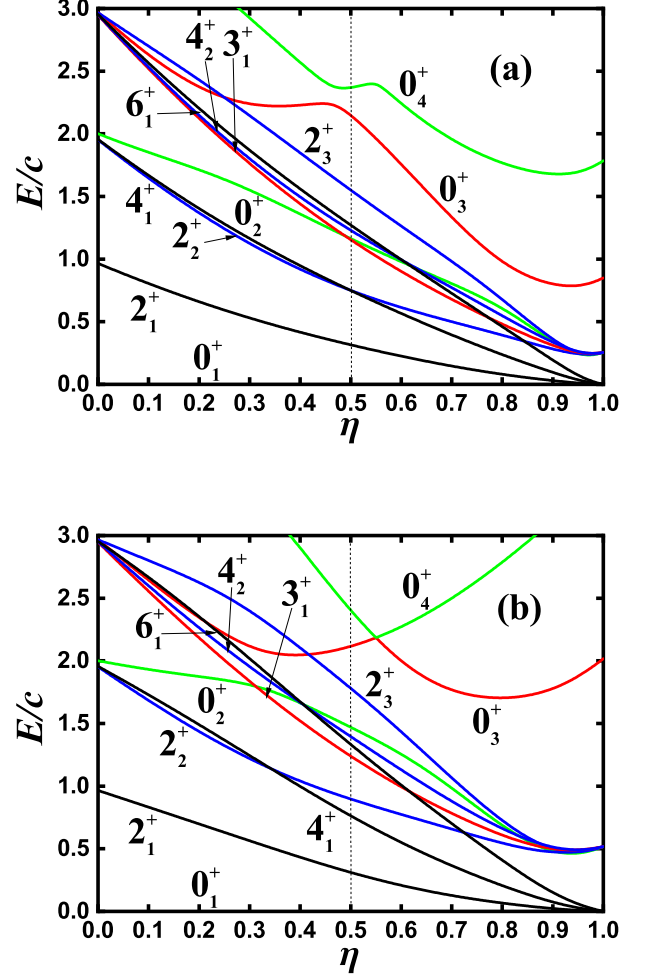


FIG. 4. Partial low-lying level evolution along the blue line in Fig. 1 for  $N = 6$  when (a)  $\xi = 0$  and (b)  $\xi = 0.05$ .

$N = 6$ . Obviously there are two crossing points between the  $4_1^+$  and  $2_2^+$  states at  $\kappa_A = 1.188$  and  $\kappa_B = 1.404$ . The position relationships of these three states are very important for understanding the  $\gamma$ -softness in realistic nuclei. The left one is the point A, and the right point is denoted by B, which is the special point discussed in this paper. The location of the point B is  $\kappa_B = 1.404$ . Point A is biased toward the prolate side and point B toward the oblate side. In the  $\gamma$ -soft-like region between the two points, point B is closest to the oblate shape.  $^{196}\text{Pt}$  is a  $\gamma$ -soft nucleus with large positive quadrupole moment, so it is natural to investigate whether the spectrum at point B can be used to describe this nucleus. It should be noticed that the value of  $\kappa_A = 1.188$  is somewhat smaller than the value of the SU(3) degenerate point 1.2, thus the real degenerate line between the U(5) limit and the SU(3) degenerate point is not the directly connected green line in Fig. 1 [23], which is also discussed in [4]. There is a sudden shape change through the SU(3) de-





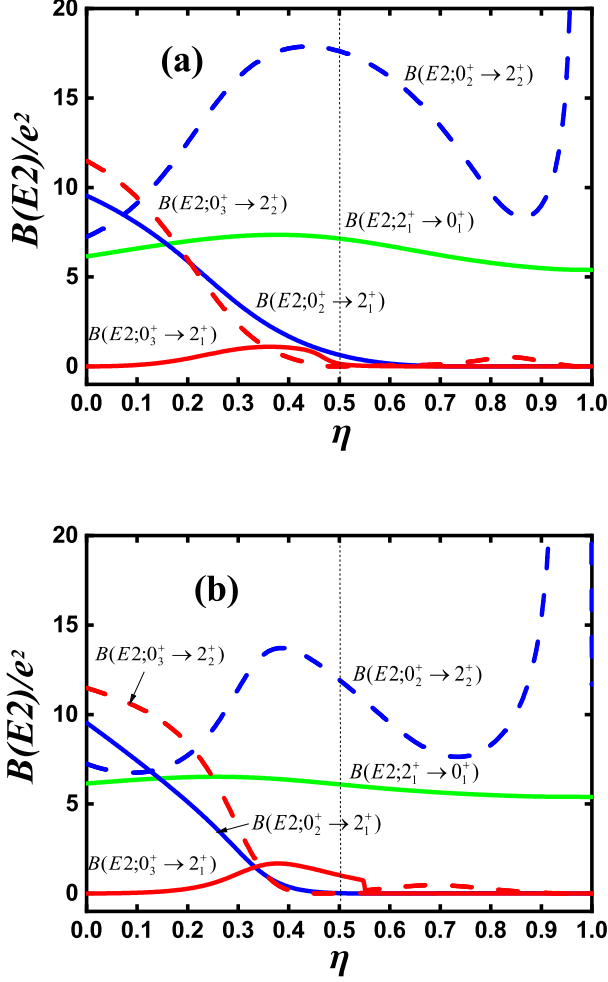


FIG. 7. The evolution of the  $B(E2; 2_1^+ \rightarrow 0_1^+)$  (green real line),  $B(E2; 0_2^+ \rightarrow 2_1^+)$  (blue real line),  $B(E2; 0_2^+ \rightarrow 2_2^+)$  (blue dashed line),  $B(E2; 0_3^+ \rightarrow 2_1^+)$  (red real line), and  $B(E2; 0_3^+ \rightarrow 2_2^+)$  (red dashed line) as the function of  $\eta$  when  $\kappa = 1.404$ , and (a)  $\xi = 0$ , (b)  $\xi = 0.05$  for  $N = 6$ .

from the two figures below. In Fig. 5 (a) the low-lying part is very similar to the vibrational spectra of a rigid spherical nucleus. The key difference is that some bands ( $0_4^+$ ,  $2_8^+$ ,  $0_6^+$  as bandheads) are greatly elevated. When moving from the point A to the point B, then with the adding of fourth-order term, the degeneracies are gradually broken and the familiar  $\gamma$ -soft feature emerges, while the regularity of the spectra is weakened.

#### IV. $B(E2)$ VALUES AND QUADRUPOLE MOMENTS FOR THE POINT B

The  $B(E2)$  values are vital for understanding the collective behaviors. In the common experiences of nuclear structure studies, we often expect a definite relationship

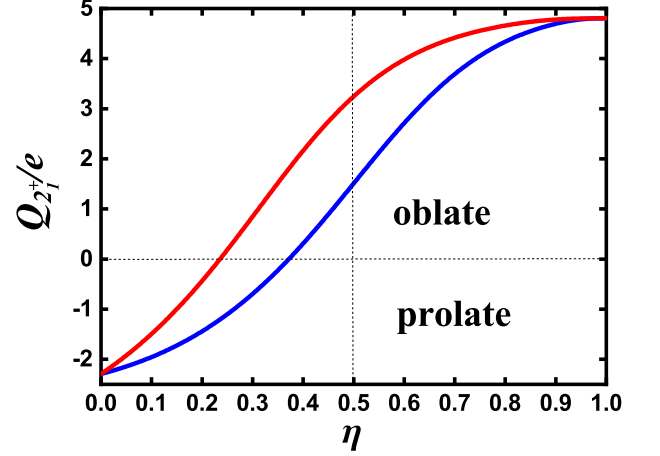


FIG. 8. The evolution of the quadrupole moment of the  $2_1^+$  state along the blue line in Fig. 1 for  $N = 6$  when  $\xi = 0$  (the solid blue line) and  $\xi = 0.05$  (the solid red line).

between the energy spectra and the corresponding  $B(E2)$  values, especially in the IBM. However this relation may lead to the wrong conclusions. In the spherical nucleus puzzle [9, 11, 12], the energy spectra of the Cd isotopes are similar to the ones of the rigid spherical vibrations, but the  $B(E2)$  values are experimentally found to violate the expectations. Thus new perspectives on the shape evolution from the magic number nucleus to the deformation need to be developed. In the  $B(E2)$  anomaly [15–18], this case becomes more obvious. From the level evolutions of the Pt-Os-W isotopes with neutron number, the energy spectra of  $^{172}\text{Pt}$ ,  $^{168,170}\text{Os}$ ,  $^{166}\text{W}$  seem normal, but their  $B(E2)$  values completely exceed expectations. Thus collective behaviors cannot be determined solely by the energy spectra. Various nuclear spectroscopic methods are needed [12].

For understanding  $\gamma$ -softness, the  $B(E2)$  values are also necessary. Especially when the new  $\gamma$ -softness is provided [1], how to distinguish the different  $\gamma$  softness becomes more and more important in the description of the realistic nuclei properties. The  $E2$  operator is defined as

$$\hat{T}(E2) = e\hat{Q}, \quad (8)$$

where  $e$  is the boson effective charge. The evolution of the  $B(E2; 2_1^+ \rightarrow 0_1^+)$ ,  $B(E2; 0_2^+ \rightarrow 2_1^+)$ ,  $B(E2; 0_2^+ \rightarrow 2_2^+)$ ,  $B(E2; 0_3^+ \rightarrow 2_1^+)$ , and  $B(E2; 0_3^+ \rightarrow 2_2^+)$  values are plotted along the blue line in Fig. 1 for  $N = 6$ . In Fig. 7 (a) the  $B(E2; 2_1^+ \rightarrow 0_1^+)$  value is nearly the same. For  $\eta = 1.0$ , it describes an oblate shape [24], thus the  $B(E2; 2_1^+ \rightarrow 0_1^+)$  value is suppressed. With the increasing of  $\eta$ , the values of  $B(E2; 0_2^+ \rightarrow 2_1^+)$  and  $B(E2; 0_3^+ \rightarrow 2_2^+)$  get reduced while the ones of the  $B(E2; 0_2^+ \rightarrow 2_2^+)$  becomes larger. The trends are similar to the ones along the green line with degeneracy and the  $\gamma$ -softness can emerge. When

the fourth-order interaction is introduced in Fig. 7 (b), at  $\eta = 0.5$ , the value of  $B(E2; 0_2^+ \rightarrow 2_2^+)$  can be reduced.

Fig. 8 shows the quadrupole moments of the  $2_1^+$  state for  $\xi = 0$  (the solid blue line) and  $\xi = 0.05$  (the solid red line). It is shown that, for the blue line, when  $\eta \geq 0.372$ , the value becomes positive, which means an oblate deformation. For the red line, it bends to the oblate side.

## V. THEORETICAL FITTING OF $^{196}\text{Pt}$

Without considering other higher-order interactions in the SU(3) limit, the properties of the point  $B$  or adding the fourth-order interaction are used to fit the structure of  $^{196}\text{Pt}$ . Although the precision needs to be improved, the fitting results seem excellent. For  $\xi = 0$  at point  $B$ , the overall energy parameter  $c$  in  $\hat{H}$  is 0.9753 MeV to make the energy value of the  $0_2^+$  state equal to the experimental one. The  $L^2$  term is also added to fit the  $2_1^+$  state, which is 0.00803 MeV. The theoretical spectra of point  $B$  shown in Fig. 9 (b) are compared with the experimental data shown in Fig. 9 (a). The theory and the experiment correspond well qualitatively, and we can see that the position relationships of each energy level are also consistent. The rotational-like  $\gamma$ -band in  $^{196}\text{Pt}$  is an interesting problem, and the theoretical spectra have similar structures.  $0_4^+$  and  $0_5^+$  states also fit well. The main drawback is that the  $0_3^+$ ,  $2_5^+$  and  $2_6^+$  are somewhat higher, that is, the energy difference between the  $0_3^+$  and  $0_2^+$  states is somewhat larger than the experimental result. This is the typical feature of the new  $\gamma$ -soft-like rotational mode [1]. For  $\xi = 0.05$ , better fitting results can be obtained, where the characteristics of the  $\gamma$  band are consistent with the actual situation and the energies of the  $0_3^+$  and  $0_4^+$  states are also reduced. For reducing the energies of the higher-levels, Pan *et al.* presented a new method to provide an excellent fitting result for  $^{194}\text{Pt}$  [58], which may be used to improve the fitting precision in the SU3-IBM.

Table I lists the  $B(E2)$  values of some low-lying states in  $^{196}\text{Pt}$ , the point  $B$  (Res.1), adding the fourth-order term (Res.2), the O(6) partial dynamical symmetry model (PDS) [57] and the modified soft-rotor model (MSR) [59]. These three models are all related to higher-order interactions in IBM. In the O(6) partial dynamical symmetry, one three-body interactions that is partially solvable in O(6) symmetry can be constructed, which can mix the  $\Sigma = 4$  and  $\Sigma = 2$ , but it does not change the case  $\Sigma = 6$  for  $N = 6$  ( $\Sigma$  is the O(6) label). In the modified soft-rotor model, the higher-order interactions are used to fit the Pt isotopes, which is inspired by the O(6) higher-order symmetry description of  $^{194}\text{Pt}$  [58]. For Res.1, this  $\gamma$ -soft-like description of the point  $B$  can show a good consistency with the experimental data qualitatively [60]. From the overall fitting results, it looks like somewhat worse than the other two theories, but the result is still good considering that the parameters of the point  $B$  are not adjustable. When the fourth-order interactions are

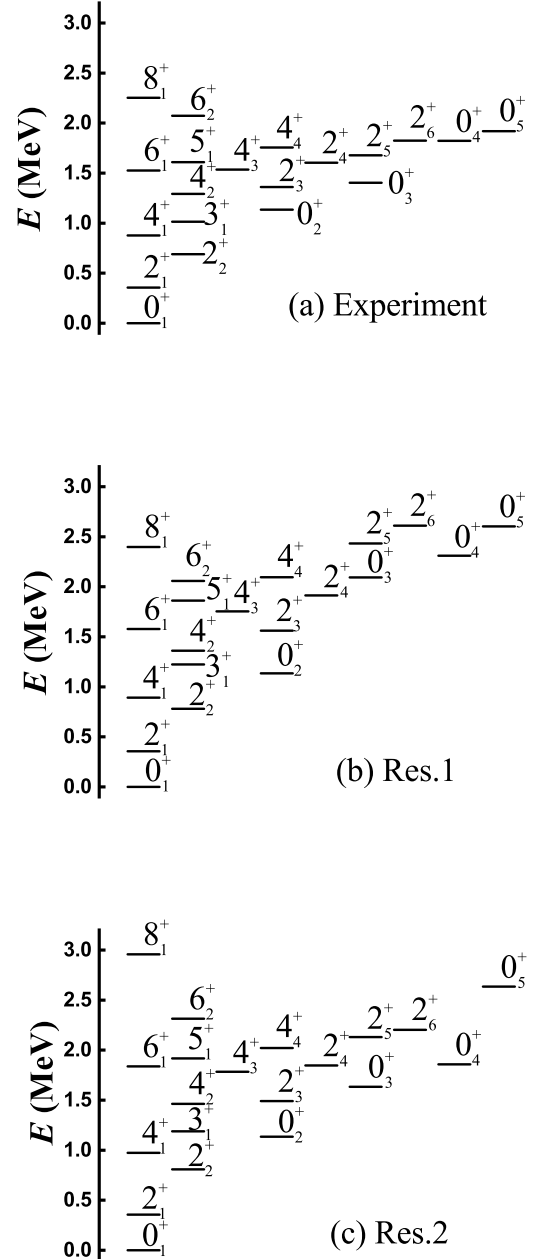


FIG. 9. Energy spectra of (a)  $^{196}\text{Pt}$ , and of the Hamiltonian in Eq. (3) at the point  $B$  (b) and when adding the fourth-order interaction when  $\xi = 0.05$  for  $N = 6$  (c).

introduced for  $\xi = 0.05$ , the fit can be greatly improved.

To better substantiate this conclusion, a quantitative analysis is mandatory. The first quantity that we might study is the staggering parameter  $S(J)$  in  $\gamma$  band energies

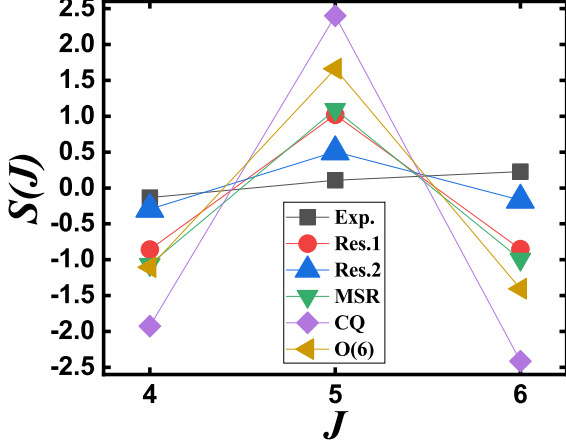


FIG. 10. The staggering parameter  $S(J)$  for  $^{196}\text{Pt}$  and various models.

TABLE I. Absolute  $B(E2)$  values in W.u. for  $E2$  transitions from the low-lying states in  $^{196}\text{Pt}$ , Res.1 for the cousin point  $B$ , Res.2 for adding the fourth-order interaction when  $\xi = 0.05$ , the PDS model and the MSR model with effective charge  $e = 2.385$  (W.u.) $^{1/2}$  for Res.1 and  $e = 2.623$  (W.u.) $^{1/2}$  for Res.2.

$L_i$	$L_f$	Exp. <sup>a</sup>	Res.1	Res.2	PDS <sup>b</sup>	MSR <sup>c</sup>
$2_1^+$	$0_1^+$	40.60(20)	40.6	40.6	40.6	40.6
$2_2^+$	$2_1^+$	54(+11 -12)	60.3	43.2	53.0	45.3
	$0_1^+$	$< 7.8 \times 10^{-6}$	2.9	5.05	0.27	1.4
$4_1^+$	$2_1^+$	60.0(9)	52.6	51.4	53.0	53.6
$0_2^+$	$2_1^+$	2.8(15)	3.6	0.122	0.44	3.1
	$2_2^+$	18(10)	100.0	79.5	54.1	69.6
$6_1^+$	$4_1^+$	73(+4 -73)	52.1	45.3	54.1	54.7
$4_2^+$	$4_1^+$	17(6)	34.4	27.4	25.8	18.1
	$2_1^+$	0.56(+12 -17)	0.65	1.34	0.14	0.69
	$2_2^+$	29(+6 -29)	38.0	31.2	28.3	28.8
$2_3^+$	$4_1^+$	0.13(12)	2.34	0.23	0.059	0.60
	$2_2^+$	0.26(23)	3.93	3.47	0.19	0.27
	$0_1^+$	0.0025(24)	0.025	0.02	0	0.064
	$0_2^+$	5(5)	38.3	36.5	17.6	0.003
$0_3^+$	$2_1^+$	$< 5.0$	0.88	6.82	0	1.05
	$2_2^+$	$< 0.41$	0.015	0.114	0.41	0.009
$6_2^+$	$6_1^+$	16(5)	23.2	17.7	15.3	9.5
	$4_1^+$	0.48(14)	0.29	0.77	0.12	0.50
	$4_2^+$	49(13)	42.1	31.9	32.7	32.9
$8_1^+$	$6_1^+$	78(+10 -78)	49.1	29.3		47.6

<sup>a</sup>From Ref.[60]

<sup>b</sup>From Ref.[57]

<sup>c</sup>From Ref.[59]

[61, 62] defined as

$$S(J) = \frac{(E_J - E_{J-1}) - (E_{J-1} - E_{J-2})}{E_{2_1^+}}, \quad (9)$$

which quantifies how adjacent levels within a  $\gamma$  band are grouped. Fig. 10 presents the  $S(J)$  for  $J = 4, 5, 6$  in ex-

TABLE II.  $R'$  and  $R$  in  $^{196}\text{Pt}$  and various models.

	Exp. <sup>a</sup>	Res.1	Res.2	MSR <sup>c</sup>	CQ <sup>c</sup>	O(6) <sup>b</sup>	PDS <sup>b</sup>
$R'$	1.236	1.845	1.440	1.131	1.281	1.543	1.786
$R$	-0.701	-0.896	-0.864	-0.192	-0.286	-0.289	-0.629

<sup>a</sup>From Ref.[60]

<sup>b</sup>From Ref.[57]

<sup>c</sup>From Ref.[59]

TABLE III. Quadrupole moments in eb and average variance  $\Delta Q$  for some low-lying states in  $^{196}\text{Pt}$  and various models.

	Exp. <sup>a</sup>	Res.1	Res.2	MSR <sup>b</sup>	CQ <sup>b</sup>
$Q(2_1^+)$	+0.62	+0.30	+0.70	+0.50	+0.40
$Q(2_2^+)$	-0.39	-0.48	-0.81	-0.47	-0.37
$Q(4_1^+)$	+1.03	+0.036	+0.63	+0.66	+0.40
$Q(6_1^+)$	-0.18	-0.42	+0.35	+0.76	+0.38
$\Delta Q$		0.54	0.39	0.51	0.44

<sup>a</sup>From Ref.[60]

<sup>b</sup>From Ref.[59]

perimental data, Res.1 and Res.2 in the SU3-IBM, MSR [59], CQ [59] and O(6) symmetry [57]. Black squares are the experimental results. CQ shows the typical  $\gamma$ -soft feature of strong staggering. O(6), MSR and Res.1 display similar trends, while Res.2 gives the best fitting.

The second is on the positions of the  $0_2^+$ ,  $0_3^+$  and  $0_4^+$  states in the spectra.  $R' = E_{0_3^+}/E_{0_2^+}$  is the energy ratio between the  $0_2^+$  and  $0_3^+$  states.  $R = E_{0_4^+}/E_{0_3^+} - 2$  is used in [57]. Table II presents the  $R'$  and  $R$  in experimental data, Res.1, Res.2, MSR [59], CQ [59], O(6) symmetry [57] and PDS [57]. For  $R'$ , Res.2, MSR and CQ can offer reasonable results. For  $R$ , Res.1, Res.2 and PDS can give the best results that are consistent with the experiment data. In [57], although the introduction of higher-order interaction can fit the  $R$  well, it increases  $R'$ . Res.2 is the only theory that makes both values more consistent. What needs to be mentioned is that the  $0_4^+$  state in  $^{194}\text{Pt}$  is an intruder state [58], thus the experimental  $0_3^+$  (or  $0_4^+$ ) state in  $^{196}\text{Pt}$  may be also an intruder state.

The experimental data about the quadrupole moments are rare, which are very sensitive to specific nuclear structure models. Table III presents the quadrupole moments of some low-lying states in  $^{196}\text{Pt}$ , which contain the results of Res.1, Res.2, the MSR model [59] and CQ [59]. The average variance of the fit  $\Delta Q$  are calculated. Our results are more consistent with the experimental data. The quadrupole moment of these states in the O(6) limit are all zero with  $\Delta Q = 0.64$ . The quadrupole moments can be a very useful indicator for judging the success of different nuclear models.

The results of these three quantitative calculations favour the description in terms of SU3-IBM over previous theories.



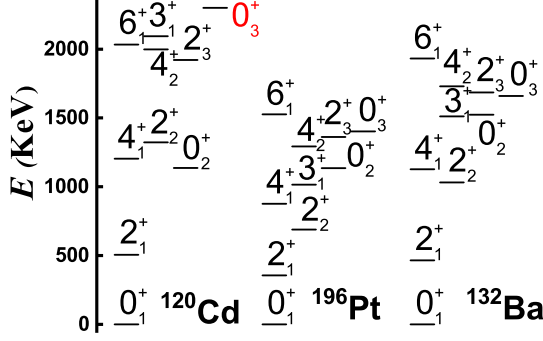


FIG. 11. Partial energy spectra in  $^{120}\text{Cd}$  normal states,  $^{196}\text{Pt}$  and  $^{132}\text{Ba}$  [65]. The energy of the  $0_3^+$  state in the  $^{120}\text{Cd}$  normal states is predicted by the authors.

## VI. SOME DISCUSSIONS ABOUT THE EMERGING $\gamma$ -SOFTNESS

The spherical nucleus puzzle [7–14] and  $B(E2)$  anomaly [15–18] dramatically change our view of nuclear structure and shape evolutions. These two peculiar phenomena occur in the collective modes of nuclei with boson number  $N < 10$ . This means that the emergence of collective motions in realistic nuclei will be a more complex problem. Even for typical large-deformation nuclei as  $^{154}\text{Sm}$  and  $^{166}\text{Er}$ , new studies have found that the structure of  $^{154}\text{Sm}$  shows the coexistence of prolate and triaxial shapes, while the deformed shape with a strong triaxial instability is demonstrated on  $^{166}\text{Er}$ , which has shown to be related with self-organization mechanism [63, 64]. Holding an obstinate simple view of collective motions in nuclei seems very undesirable. Further experimental information on the two puzzles may lead us to get a more accurate description on nuclear structures.

This article can be seen as an extension of the previous works [1, 4]. In these papers, the SU3-IBM is proposed, which is inspired by the interesting findings in Ref. [23, 24]. When only the U(5) limit and the SU(3) limit are concerned,  $\gamma$ -soft-like rotational mode can also occur as an emergent phenomenon if the SU(3) higher-order interactions are introduced into the common formalism. This is very different from the  $\gamma$ -softness related to the O(6) limit. In the traditional IBM, O(6) symmetry is exactly solvable, and  $\gamma$ -unstable spectra can be expected. Especially the SU3-IBM can describe the  $B(E2)$  anomaly, which make the model particularly useful.

Fig. 11 presents partial energy spectra of  $^{120}\text{Cd}$ ,  $^{196}\text{Pt}$  and  $^{132}\text{Ba}$ , for their boson number are all  $N = 6$ . Ref. [10] obtains the spectra of  $^{120}\text{Cd}$ , in which the  $0_3^+$  state at the three-phonon level is absent. The energy of the  $0_3^+$  state of  $^{120}\text{Cd}$  is predicted by our theory, which is around 2300 KeV, or even higher. Thus this is really

a new  $\gamma$ -soft rotational mode [8, 9, 12], despite it looks much like the rigid spherical vibrational excitation mode. If we consider that the IBM can truly describe the collective excitations in realistic nuclei, the only way to describe the new  $\gamma$ -soft behaviors is to introduce the SU(3) higher-order interactions. The theory works better than expected [1–3].

$^{196}\text{Pt}$  and  $^{132}\text{Ba}$  are two typical traditional  $\gamma$ -soft nuclei. In the IBM, this kind of  $\gamma$ -softness is related to the O(6) symmetry, or O(5) symmetry, such as E(5) critical point description [66, 67]. In fact, this case is not related to the deformation  $\gamma$  parameter. The SU3-IBM follows such a principle that triaxiality arises from the competition between the prolate shape and the oblate shape. In this paper, we show that the new emerging  $\gamma$ -softness can resemble the traditional  $\gamma$ -soft spectra and their  $B(E2)$  behaviors. When other SU(3) higher-order interactions are introduced, the fitting of spectra appears excellent. This will be further discussed in following papers.

In previous discussions, spectra and low-lying  $B(E2)$  values of various  $\gamma$ -soft rotational modes in different nuclear structure theories are very similar, so distinguishing various  $\gamma$ -softness in different theories is becoming extremely important. New  $\gamma$ -softness in the normal states of Cd nuclei can be only described by the SU3-IBM. However the spherical nucleus puzzle is still full of debates [13, 14, 68, 69]. A complete description of  $^{110,112}\text{Cd}$  including configuration mixing, like Ref. [70–74], is in progress.  $B(E2)$  values between higher levels are useful, such as the  $0_3^+$ ,  $2_4^+$  and  $2_5^+$  states. Quadrupole moments of the low-lying states may provide great value in distinguishing among the various models.

Though a lot of theoretical work still needs to be done, we expect that many observations in  $\gamma$ -soft-like nuclei might be described by the SU3-IBM in a unified way. E(5)-like  $\gamma$ -softness in  $^{82}\text{Kr}$  is found in the new model [5]. Each interaction in the SU3-IBM has a clear geometric meaning, and different from common considerations in microscopic theory, such as SD-pair shell model [75, 76]. In the microscopic theory, various deformations resulting from the proton-neutron interactions can give rise to different deformation shapes, including the  $\gamma$ -soft rotational mode [77, 78]. In the SU3-IBM, this is not so, and specific interaction corresponds to certain shape, and the  $\gamma$ -softness is an emergent phenomenon, which can not be expected before numerical calculations. How to understand this point is an interesting problem. From the existing results, the SU3-IBM is closer to the geometric collective model [50]. It seems important to investigate further the emerging  $\gamma$ -softness in the geometric model [79, 80].

Since the seminal works by Elliott [81–83], the SU(3) symmetry has played a key role for the description of the rotational spectra from the perspective of a microscopic shell model [35, 84–96]. It was also found that the SU(3) symmetry plays a key role in the description of shell-like quartetting of nucleons, and the SU(3) third-order Casimir operator  $\hat{C}_3[\text{SU}(3)]$  is needed to describe the ex-

perimental spectra in order to distinguish between the prolate and oblate shapes [97–100]. In the previous studies, the SU(3) symmetry has been related to the prolate shape. In our new findings ([1–6] and this paper), the SU(3) symmetry actually dominates all the quadrupole deformations. In particular, in this model, one can obtain large quadrupole moments, even with spectra that resemble a gamma-soft situation. We expect that this new perspective can be further used in the SU(3) shell model [87, 88].

Along the dashed red line through the  $A$  and  $B$  point, shape phase transition from the prolate shape to the oblate shape has been studied [4], and this is an asymmetric evolution, which is different from the symmetric one in  $\hat{H}_1$  [101, 102]. The study of the properties of  $^{196}\text{Pt}$  in this paper further supports this perspective and a more detailed investigation on the prolate-oblate shape phase transition is also needed.

In addition, in Ref. [5], the E(5)-like energy spectrum was also found in the new model, where there are also some new findings pointing to the  $\gamma$ -softness, which are further used to understand the  $^{196}\text{Pt}$ , which will be given in the second part (II) of the discussions.

Rigid triaxial rotor in nuclear structure was first studied by Davydov and Filippov [104]. In the SU(3) shell model, a SU(3) mapping of the rigid triaxial rotor can be obtained, which bridges between the geometrical model and the shell model [105–107]. This SU(3) mapping was also discussed in the IBM [30, 31]. Twenty years ago Wood *et al.* investigated the triaxial rotor model by relaxing the use of irrotational moments of inertia [108]. Then this model was used to describe the  $E2$  matrix elements available for  $^{186,188,190,192}\text{Os}$  [109], which were usually treated as  $\gamma$ -soft nuclei. Importantly, the nearly zero value of the B(E2) transition from the  $2_2^+$  state to the  $0_1^+$  state in  $^{196}\text{Pt}$  can be explained by this model. These can help us further improve the fitting effect of  $^{196}\text{Pt}$ .

In the SU(3) mapping,  $[\hat{L} \times \hat{Q} \times \hat{L}]^{(0)}$ ,  $[(\hat{L} \times \hat{Q})^{(1)} \times (\hat{L} \times \hat{Q})^{(1)}]^{(0)}$  and  $\hat{L}^2$  are used to describe the rotational spectrum of the rigid triaxial rotor, but they can not affect the positions of the  $0^+$  states. In this paper, it is shown that the  $0^+$  states can be well explained by introducing the SU(3) third-order  $\hat{C}_3[\text{SU}(3)]$  and the forth-order interactions  $\hat{C}_2^2[\text{SU}(3)]$ . Thus introducing the  $[\hat{L} \times \hat{Q} \times \hat{L}]^{(0)}$  and  $[(\hat{L} \times \hat{Q})^{(1)} \times (\hat{L} \times \hat{Q})^{(1)}]^{(0)}$  will further improve the fitting effect of the B(E2) values in Table I. A SU(3) mapping of the works done by Wood *et al.* [108–110] will be first needed. These will be given in the third and forth parts (III, IV) of the discussions.

## VII. CONCLUSIONS

Recently, the interacting boson model with SU(3) higher-order interactions (SU3-IBM) was proposed [1–3] to resolve the spherical nucleus puzzle [8–14], the  $B(E2)$  anomaly [15–18] and the prolate-oblate shape asymmetric evolution [4, 101, 102]. Although this model can be obtained by only considering the U(5) limit and the SU(3) limit, the  $\gamma$ -soft-like rotational mode can emerge. These results may extend our view of the interacting boson model (IBM). As said by Heyde and Wood: “sphericity is a special case of deformation.” and “the reference frame must be fundamentally one of a deformed many-body system.” [11]. The emerging  $\gamma$ -softness may play a key role in the shift of perspective.

Following the previous studies [1, 4], the emerging  $\gamma$ -soft-like rotational mode can be explored to explain the properties of  $^{196}\text{Pt}$ . In our studies, a special point, which is near the middle point of the degenerate line connected the U(5) limit and the SU(3) degenerate point, is explored. The purpose of this paper is only to explore the relationship between the emerging  $\gamma$ -softness and the  $\gamma$ -soft properties in realistic nuclei. Further detailed fitting will be done in future when other SU(3) higher-order interactions are introduced, which is related to the destructive interference effect in the triaxial rotor model [108–110].

Further investigation of the  $\gamma$ -rigid triaxiality is also important in the SU3-IBM. This is a delicate topic [48]. The phase diagram of the SU3-IBM will be given in future, and it can offer meaningful guidance to the rigid triaxiality. 6- $d$  interaction may be also valuable [27, 28]. Distinguishing between the different  $\gamma$ -softness and discussing the differences between the  $\gamma$ -softness and the rigid triaxiality are topics that require further exploration.

Finally, a direct discussion and fitting of the new model on the oblate nuclei, such as  $^{196-204}\text{Hg}$ , is no doubt extremely important for understanding the SU3-IBM and for establishing the relationship between the new model and the SU(3) shell model.

## VIII. ACKNOWLEDGMENT

This research is supported by the Educational Department of Jilin Province, China (JJKH20210526KJ). C.-x.Z. gratefully acknowledges support from the Project Supported by Scientific Research Fund of Hunan Provincial Education Department, China (21A0427).

- 
- [1] T. Wang, Chin. Phys. C **46**, 074101 (2022).
  - [2] T. Wang, EPL **129**, 52001 (2020).
  - [3] Y. Zhang, Y. W. He, D. Karlsson, C. Qi, F. Pan and J. P. Draayer, Phys. Lett. B **834**, 137443 (2022).

- [4] T. Wang, B. C. He, D. K. Li and C. X. Zhou, Phys. Rev. C **78**, 064322 (2023).
- [5] C. X. Zhou and T. Wang, Phys. Rev. C **108**, 024309 (2023).

- [6] T. Wang, Phys. Rev. C **107**, 064303 (2023).
- [7] P. E. Garrett, K. L. Green and J. L. Wood, Phys. Rev. C **78**, 044307 (2008).
- [8] P. E. Garrett and J. L. Wood, J. Phys. G: Nucl. Part. Phys. **37**, 064028 (2010).
- [9] P. E. Garrett, J. Bangay, A. Diaz Varela, G. C. Ball, D. S. Cross, G. A. Demand, P. Finlay, A. B. Garnsworthy, K. L. Green, G. Hackman, C. D. Hannant, B. Jigmeddorj, J. Jolie, W. D. Kulp, K. G. Leach, J. N. Orce, A. A. Phillips, A. J. Radich, E. T. Rand, M. A. Schumaker, C. E. Svensson, C. Sumithrarachchi, S. Triambak, N. Warr, J. Wong, J. L. Wood and S. W. Yates, Phys. Rev. C **86**, 044304 (2012).
- [10] J. C. Batchelder, N. T. Brewer, R. E. Goans, R. Grzywacz, B. O. Griffith, C. Jost, A. Korgul, S. H. Liu, S. V. Paulauskas, E. H. Spejewski and D. W. Stracener, Phys. Rev. C **86**, 064311 (2012).
- [11] K. Heyde and J. L. Wood, Phys. Scr. **91**, 083008 (2016).
- [12] P. E. Garrett, J. L. Wood and S. W. Yates, Phys. Scr. **93**, 063001 (2018).
- [13] P. E. Garrett, Rodríguez, A. Diaz Varela, K. L. Green, J. Bangay, A. Finlay, R. A. E. Austin, G. C. Ball, D. S. Bandyopadhyay, V. Bildstein, S. Colosimo, D. S. Cross, G. A. Demand, P. Finlay, A. B. Garnsworthy, G. F. Grinyer, G. Hackman, B. Jigmeddorj, J. Jolie, W. D. Kulp, K. G. Leach, A. C. Morton, J. N. Orce, C. J. Pearson, A. A. Phillips, A. J. Radich, E. T. Rand, M. A. Schumaker, C. E. Svensson, C. Sumithrarachchi, S. Triambak, N. Warr, J. Wong, J. L. Wood and S. W. Yates, Phys. Rev. Lett. **123**, 142502 (2019).
- [14] P. E. Garrett, Rodríguez, A. Diaz Varela, K. L. Green, J. Bangay, A. Finlay, R. A. E. Austin, G. C. Ball, D. S. Bandyopadhyay, V. Bildstein, S. Colosimo, D. S. Cross, G. A. Demand, P. Finlay, A. B. Garnsworthy, G. F. Grinyer, G. Hackman, B. Jigmeddorj, J. Jolie, W. D. Kulp, K. G. Leach, A. C. Morton, J. N. Orce, C. J. Pearson, A. A. Phillips, A. J. Radich, E. T. Rand, M. A. Schumaker, C. E. Svensson, C. Sumithrarachchi, S. Triambak, N. Warr, J. Wong, J. L. Wood and S. W. Yates, Phys. Rev. C **101**, 044302 (2020).
- [15] T. Grahn, S. Stolze, D. T. Joss, R. D. Page, B. Saygı, D. O'Donnell, M. Akmali, K. Andgren, L. Bianco, D. M. Cullen, A. Dewald, P. T. Greenlees, K. Heyde, H. Iwasaki, U. Jakobsson, P. Jones, D. S. Judson, R. Julin, S. Juutinen, S. Ketelhut, M. Leino, N. Lumley, P. J. R. Mason, O. Möller, K. Nomura, M. Nyman, A. Petts, P. Peura, N. Pietralla, T. Pissulla, P. Rahkila, P. J. Sapple, J. Sarén, C. Scholey, J. Simpson, J. Sorri, P. D. Stevenson, J. Uusitalo, H. V. Watkins and J. L. Wood, Phys. Rev. C **94**, 044327 (2016).
- [16] B. Saygı, D. T. Joss, R. D. Page, T. Grahn, J. Simpson, D. O'Donnell, G. Alharshan, K. Auranen, T. Bäck, S. Boening, T. Braunroth, R. J. Carroll, B. Cederwall, D. M. Cullen, A. Dewald, M. Doncel, L. Donosa, M. C. Drummond, F. Ertuğral, S. Ertürk, C. Fransen, P. T. Greenlees, M. Hackstein, K. Hauschild, A. Herzan, U. Jakobsson, P. M. Jones, R. Julin, S. Juutinen, J. Konki, T. Kröll, M. Labiche, A. Lopez-Martens, C. G. McPeake, F. Moradi, O. Möller, M. Mustafa, P. Nieminen, J. Pakarinen, J. Partanen, P. Peura, M. Procter, P. Rahkila, W. Rother, P. Ruotsalainen, M. Sandzelius, J. Sarén, C. Scholey, J. Sorri, S. Stolze, M. J. Taylor, A. Thornthwaite and J. Uusitalo, Phys. Rev. C **96**, 021301(R) (2017).
- [17] B. Cederwall, M. Doncel, Ö. Aktas, A. Ertoprak, R. Liotta, C. Qi, T. Grahn, D. M. Cullen, B. S. Nara Singh, D. Hodge, M. Giles, S. Stolze, H. Badran, T. Braunroth, T. Calverley, D. M. Cox, Y. D. Fang, P. T. Greenlees, J. Hilton, E. Ideguchi, R. Julin, S. Juutinen, M. K. Raju, H. Li, H. Liu, S. Matta, V. Modamio, J. Pakarinen, P. Papadakis, J. Partanen, C. M. Petrache, P. Rahkila, P. Ruotsalainen, M. Sandzelius, J. Sarén, C. Scholey, J. Sorri, P. Subramaniam, M. J. Taylor, J. Uusitalo and J. J. Valiente-Dobón, Phys. Rev. Lett. **121**, 022502 (2018).
- [18] A. Goasduff, J. Ljungvall, T. R. Rodríguez, F. L. Bello Garrote, A. Etile, G. Georgiev, F. Giacompo, L. Grente, M. Klintefjord, A. Kusoğlu, I. Matea, S. Roccia, M.-D. Salsac and C. Sotty, Phys. Rev. C **100**, 034302 (2019).
- [19] A. Arima and F. Iachello, Phys. Rev. Lett. **40**, 385 (1978).
- [20] F. Iachello and A. Arima, *The Interacting Boson Model*, (Cambridge University Press, Cambridge, 1987).
- [21] P. Cejnar, J. Jolie and R. F. Casten, Rev. Mod. Phys. **82**, 2155 (2010).
- [22] F. Pan, T. Wang, Y. S. Huo and J. P. Draayer, J. Phys. G: Nuclear and Particle Physics **35**, 1263 (2008).
- [23] L. Fortunato, C. E. Alonso, J. M. Arias, J. E. García-Ramos and A. Vitturi, Phys. Rev. C **84**, 014326 (2011).
- [24] Y. Zhang, F. Pan, Y. X. Liu, Y. A. Luo and J. P. Draayer, Phys. Rev. C **85**, 064312 (2012).
- [25] R. F. Casten, Nat. Phys. **2**, 811 (2006).
- [26] K. Heyde and J. L. Wood, Rev. Mod. Phys. **83**, 1467 (2011).
- [27] P. Van Isacker and J. Q. Chen, Phys. Rev. C **24**, 684 (1981).
- [28] K. Heyde, P. Van Isacker, M. Waroquier and J. Moreau, Phys. Rev. C **29**, 1420 (1984).
- [29] G. Vanden Berghe, H. E. De Meyer and P. Van Isacker, Phys. Rev. C **32**, 1049 (1985).
- [30] Y. F. Smirnov, N. A. Smirnova and P. Van Isacker, Phys. Rev. C **61**, 041302(R) (2000).
- [31] Y. Zhang, F. Pan, L. R. Dai and J. P. Draayer, Phys. Rev. C **90**, 044310 (2014).
- [32] G. Rosensteel and D. J. Rowe, Ann. Phys. (N.Y.) **104**, 134 (1977).
- [33] J. P. Draayer and G. Rosensteel, Nucl. Phys. A **439**, 61 (1985).
- [34] J. P. Elliott, J. A. Evans and P. Van Isacker, Phys. Rev. Lett. **57**, 1124 (1986).
- [35] V. K. B. Kota, *SU(3) Symmetry in Atomic Nuclei*, (Springer Nature, Singapore, 2020).
- [36] A. Leviatan, Prog. Part. Nucl. Phys. **66**, 93 (2011).
- [37] P. Van Isacker, Phys. Rev. Lett. **83**, 4269 (1999).
- [38] D. J. Rowe and G. Thiamova, Nucl. Phys. A **760**, 59 (2005).
- [39] L. R. Dai, F. Pan, L. Liu, L. X. Wang and J. P. Draayer, Phys. Rev. C **86**, 034316 (2012).
- [40] L. Wilets and M. Jean, Phys. Rev. **102**, 788 (1956).
- [41] J. A. Cizewski, R. F. Casten, G. J. Smith, M. L. Stelts and W. R. Kane, Phys. Rev. Lett. **40**, 167 (1978).
- [42] M. P. Fewell, G. J. Gyapong, R. H. Spear, M. T. Esat, A. M. Baxter and S. M. Burnett, Phys. Lett. B **353**, 157 (1985).
- [43] R. F. Casten and J. A. Cizewski, Phys. Lett. B **185**, 293 (1987).
- [44] A. E. L. Dieperink and R. Bijker, Phys. Lett. B **116**, 77 (1982).

- [45] J. M. Arias, J. E. García-Ramos and J. Dukelsky, Phys. Rev. Lett. **93**, 212501 (2004).
- [46] M. A. Caprio and F. Iachello, Phys. Rev. Lett. **93**, 212501 (2004).
- [47] M. A. Caprio and F. Iachello, Ann. Phys. **318**, 454 (2005).
- [48] K. Nomura, N. Shimizu, D. Vretenar, T. Nikšić and T. Otsuka, Phys. Rev. Lett. **108**, 132501 (2012).
- [49] P. Van Isacker, A. Boudjedri and S. Zerguine, Nucl. Phys. A **836**, 225 (2010).
- [50] A. Bohr and B. R. Mottelson, *Nuclear Structure Vol. II*, (Benjamin, New York, 1975).
- [51] P. Ring and P. Schuck, *The Nuclear Many-Body Problem*, (Springer-Verlag, Berlin, 1980).
- [52] M. Bender, P.-H. Heenen and P.-G. Reinhard, Rev. Mod. Phys. **75**, 121 (2003).
- [53] E. Caurier, G. Martínez-Pinedo, F. Nowack, A. Poves and A. P. Zuker, Rev. Mod. Phys. **77**, 427 (2005).
- [54] T. Nikšić, D. Vretenar and P. Ring, Prog. Part. Nucl. Phys. **66**, 519 (2011).
- [55] N. Shimizu, T. Abe, Y. Tsunoda, Y. Utsuno, T. Yoshida, T. Mizusaki, M. Honma and T. Otsuka, Prog. Theor. Exp. Phys. **2012**, 01A205 (2012).
- [56] K. Nomura, D. Vretenar, Z. P. Li and J. Xiang, Phys. Rev. C **104**, 024323 (2021).
- [57] J. E. García-Ramos, A. Leviatan and P. Van Isacker, Phys. Rev. Lett. **102**, 112502 (2009).
- [58] F. Pan, S. L. Yuan, Z. Qiao, J. Bai, Y. Zhang and J. P. Draayer, Phys. Rev. C **97**, 034326 (2018).
- [59] D. K. Li, T. Wang and F. Pan, Symmetry **14**, 2610 (2022).
- [60] X. L. Huang, Nuclear Data Sheets **108**, 1093 (2007).
- [61] N.V. Zamfir and R.F. Casten, Phys. Lett. B **260**, 265 (1991).
- [62] E. A. McCutchan, D. Bonatsos, N. V. Zamfir and R. F. Casten, Phys. Rev. C **76**, 024306 (2007).
- [63] T. Otsuka, Y. Tsunoda, T. Abe, N. Shimizu and P. Van Duppen, Phys. Rev. Lett. **123**, 222502 (2019).
- [64] T. Otsuka, Physics **4**, 258 (2022).
- [65] ENSDF: <https://www.nndc.bnl.gov/ensdf/>
- [66] F. Iachello, Phys. Rev. Lett. **85**, 3580 (2000).
- [67] Y. Zhang, Z. T. Wang, H. D. Jiang and X. Chen, Symmetry **14**, 2219 (2022).
- [68] K. Nomura and J. Jolie, Phys. Rev. C **98**, 024303 (2018).
- [69] A. Leviatan, N. Gavrielov, J. E. García-Ramos and P. Van Isacker, Phys. Rev. C **98**, 031302(R) (2018).
- [70] J. E. García-Ramos, V. Hellemans and K. Heyde, Phys. Rev. C **84**, 014331 (2011).
- [71] N. Gavrielov, A. Leviatan and F. Iachello, Phys. Rev. C **99**, 064324 (2019).
- [72] J. E. García-Ramos and K. Heyde, Phys. Rev. C **100**, 044315 (2019).
- [73] J. E. García-Ramos and K. Heyde, Phys. Rev. C **102**, 054333 (2020).
- [74] N. Gavrielov, A. Leviatan and F. Iachello, Phys. Rev. C **105**, 014305 (2022).
- [75] Y. A. Luo and J. Q. Chen, Phys. Rev. C **58**, 589 (1998).
- [76] Y. M. Zhao, N. Yoshinaga, S. Yamaji, J. Q. Chen and A. Arima, Phys. Rev. C **62**, 014304 (2000).
- [77] Y. A. Luo, Y. Zhang, X. F. Meng, F. Pan and J. P. Draayer, Phys. Rev. C **80**, 014311 (2009).
- [78] B. C. He, S. Y. Zhang, Y. Zhang, Y. A. Luo, F. Pan and J. P. Draayer, Eur. Phys. J. A **55**, 143 (2019).
- [79] L. Fortunato, Eur. Phys. J. A, **26**, 1 (2005)
- [80] P. Baganu and L. Fortunato, J. Phys. G, **43**, 093003 (2016).
- [81] J. P. Elliott, Proc. Roy. Soc. Ser. A **245**, 128 (1958).
- [82] J. P. Elliott, Proc. Roy. Soc. Ser. A **245**, 562 (1958).
- [83] M. Harvey, Adv. Nucl. Phys. **1**, 67 (1968).
- [84] R. D. R. Raju, J. P. Draayer and K. T. Hecht, Nucl. Phys. A **202**, 433 (1973).
- [85] J. P. Draayer and K. J. Weeks, Phys. Rev. Lett. **51**, 1422 (1983).
- [86] J. P. Draayer and K. J. Weeks, Ann. Phys. **156**, 41 (1984).
- [87] C. Bahri, J. Escher and J. P. Draayer, Nucl. Phys. A **592**, 171 (1995).
- [88] G. Popa, J. G. Hirsch and J. P. Draayer, Phys. Rev. C **62**, 064313 (2000).
- [89] G. Rosensteel and D. J. Rowe, Phys. Rev. Lett. **38**, 10 (1977).
- [90] G. Rosensteel and D. J. Rowe, Ann. Phys. **126**, 343 (1980).
- [91] T. Dytrych, K. D. Sviratcheva, C. Bahri, J. P. Draayer and J. P. Vary, Phys. Rev. Lett. **98**, 162503 (2007).
- [92] T. Dytrych, K. D. Sviratcheva, C. Bahri, J. P. Draayer and J. P. Vary, Phys. Rev. C **76**, 014315 (2007).
- [93] A. P. Zuker, J. Retamosa, A. Poves and E. Caurier, Phys. Rev. C **52**, R1741 (1995).
- [94] A. P. Zuker, A. Poves, F. Nowacki and S. M. Lenzi, Phys. Rev. C **92**, 024320 (2015).
- [95] D. Bonatsos, I. E. Assimakis, N. Minkov, A. Martinou, S. Sarantopoulou, R. B. Cakirli, R. F. Casten, K. Blaum, Phys. Rev. C **95**, 064326 (2017).
- [96] D. Bonatsos, A. Martinou, S. K. Peroulis, T. J. Mertzimekis, N. Minkov, Symmetry **15**, 169 (2023).
- [97] J. Cseh, Phys. Lett. B **743**, 213 (2015).
- [98] J. Cseh and G. Riczu, Phys. Lett. B **757**, 312 (2016).
- [99] J. Cseh, Phys. Rev. C **103**, 064322 (2021).
- [100] J. Cseh, G. Riczu and J. Darai, Symmetry **15**, 115 (2023).
- [101] J. Jolie, R. F. Casten, P. von Brentano and V. Werner, Phys. Rev. Lett. **87**, 162501 (2001).
- [102] J. Jolie and A. Linnemann, Phys. Rev. C **68**, 031301(R) (2003).
- [103] C. X. Zhou, T. Wang and D. K. Li, in preparation.
- [104] A. S. Davydov and G. F. Filippov, Nucl. Phys. **8**, 237 (1958).
- [105] Y. Leschber and J. P. Draayer, Phys. Lett. B **190**, 1 (1987).
- [106] O. Castaños, J. P. Draayer and Y. Leschber, Com. Phys. Comm. **52**, 71 (1988).
- [107] O. Castaños, J. P. Draayer and Y. Leschber, Z. Phys. A **329**, 33 (1988).
- [108] J. L. Wood, A.-M. Oros-Peusquens, R. Zaballa, J. M. Allmond and W. D. Kulp, Phys. Rev. C **70**, 024308 (2004).
- [109] J. M. Allmond, R. Zaballa, A. M. Oros-Peusquens, W. D. Kulp and J. L. Wood, Phys. Rev. C **78**, 014302 (2008).
- [110] J. M. Allmond, J. L. Wood and W. D. Kulp, Phys. Rev. C **81**, 051305(R) (2010).